



130 years of heavy metal pollution archived in the shell of the intertidal dog whelk, *Nucella lapillus* (Gastropoda, Muricidae)

Dennis Mayk^{a,b,*}, Elizabeth M. Harper^{a,b}, Jan Fietzke^c, Thierry Backeljau^{d,e}, Lloyd S. Peck^a

^a Department of Earth Sciences, University of Cambridge, Downing Street, Cambridge CB2 3EQ, United Kingdom

^b British Antarctic Survey, High Cross, Madingley Road, Cambridge CB3 0ET, United Kingdom

^c Geomar, Helmholtz Center for Ocean Research, Kiel, Germany

^d Royal Belgian Institute of Natural Sciences, Brussels, Belgium

^e Evolutionary Ecology Group, University of Antwerp, Antwerp, Belgium

ARTICLE INFO

Keywords:

Museum collections
Environmental monitoring
Pollution management
Sewage
Lead emission

ABSTRACT

Heavy metals in coastal waters are a great environmental concern in the North Sea since the middle of the 20th century. Regulatory efforts have led to a significant reduction in atmospheric and water-transported heavy metals. Still, high concentrations of these in sediments remain a risk for ecosystems, requiring close monitoring. Here, we investigated the applicability of *Nucella lapillus* museum collections as a tool for targeted tracking of chronic anthropogenic heavy metal pollution. We analysed the concentration ratios of the common heavy metals Cu, Cd, Pb, and Zn in relation to Ca in *N. lapillus* shells collected from the Dutch and Belgian intertidal zone over the last 130 years. We found that shell Cu/Ca and Zn/Ca concentration ratios remained remarkably constant, whereas Pb/Ca concentration trends were closely aligned with emissions of leaded petrol in Europe. Our results suggest that *N. lapillus* provides a suitable Pb pollution archive of the intertidal zone.

1. Introduction

With more than three billion people worldwide living within 100 km of an oceanic coast (CIESIN, 2012), many industrialised and urbanised areas are close to coastal waters, which are thus often exposed to high degrees of artificially introduced pollutants. As the border between land and ocean, the intertidal zone is among the most anthropogenically impacted habitats in the world. It is influenced by immediate anthropogenic actions such as tourism and ship traffic and constitutes a high-risk area for chronic pollution from distant inland sites through riverine or atmospheric input. This chronic pollution can remain a risk to the ecosystem even after removing the source as pollutants accumulated in the sediment (Gu, 2018; Silva et al., 2017) can be resuspended into the water column by bioturbation, tidal movement or dredging activity years later (Zoumis et al., 2001). Heavy metals, i.e., metallic elements with a high density compared to water (Fergusson, 1990), are one type of pollutants that have caused increasing ecological and global public health concerns (Chitrakar et al., 2019; Tchounwou et al., 2012). Large amounts of potentially toxic metals have been released into the oceans (Dethlefsen, 1988) from, among other sources, historical waste management, unregulated coal burning, and petrol combustion, as well as

industrial discharge from mining, smelting, and chemical processing sites. For example, sediments in the Southern Bight of the North Sea were shown to contain worryingly high concentrations of the heavy metals copper (Cu), zinc (Zn), lead (Pb), and cadmium (Cd) (Baeyens, 1997; Van Alsenoy et al., 1993; Zwolsman et al., 1997) as a result of mismanaged anthropogenic effluent and industrial waste discharge, the unregulated release of combustion fumes and increasing ship traffic. One study even suggested that the Southern North Sea was one of the most oil-polluted marine areas in the world (Camphuysen and Vollaard, 2016), with the first reports of oil spills already being published in the early 20th century (Verwey, 1915). Although a substantial body of literature highlights the negative effects of heavy metal accumulation on marine biodiversity (Chitrakar et al., 2019) and consequent threats to human health (Liu et al., 2018), little is known about long-term effects on community structures, single populations or species from the near-shore. Marine organisms exposed to heavy metal pollution, such as the economically important foundation species *Mytilus edulis* and *Perna viridis* have been shown to contain high and varying levels of tissue heavy metal concentrations (Knopf et al., 2020; Ragi et al., 2017), but long-term records of these intertidal species are sparse mainly due to a lack of suitable sample material. Soft tissues are seldom suitable for

* Corresponding author at: British Antarctic Survey, High Cross, Madingley Road, Cambridge CB3 0ET, United Kingdom.

E-mail address: dennis.mayk@cantab.net (D. Mayk).

<https://doi.org/10.1016/j.marpolbul.2022.114286>

Received 21 June 2022; Received in revised form 18 October 2022; Accepted 19 October 2022

Available online 30 October 2022

0025-326X/© 2022 The Authors. Published by Elsevier Ltd. This is an open access article under the CC BY license (<http://creativecommons.org/licenses/by/4.0/>).

long-term monitoring of environmental pollution, but calcium carbonate (CaCO₃) hard parts such as shells or skeletons have been successfully used to reconstruct long-term heavy metal concentrations of off-shore sites, predominantly in the long-lived *Arctica islandica* (Holland et al., 2014; Krause-Nehring et al., 2012) and in foraminifera (Boehnert et al., 2020; Oron et al., 2021; Titelboim et al., 2021, 2018). This is possible because heavy metals, especially those exhibiting divalent cations, are incorporated in trace amounts into the crystal lattice of CaCO₃ skeletons of marine organisms, providing important archives that enable us to study the heavy metal content of samples from past environments.

In this study, we aim to add to this knowledge by presenting a 130 years record of concentrations of the common heavy metals Cu, Zn, Pb and Cd, which have a known pollution history in the Southern North Sea, from the Dutch and Belgian coast at sites near the Scheldt Estuary. We analysed the concentration ratios of these heavy metals in archival shells of the intertidal snail *Nucella lapillus* (Linnaeus, 1758) and assessed the use of such museum collections as a novel sample archive for a targeted investigation of historical heavy metal pollution levels in the intertidal zone. *Nucella lapillus* is an important predator of North Atlantic rocky shores (Burrows and Hughes, 1989; Morgan, 1972) that is widely abundant from Iceland to Portugal (Mayk et al., 2022) and exerts a strong top-down control on intertidal ecosystems (Trussell et al., 2003). Its wide geographical abundance and position in the intertidal food web make it an ideal organism to study and potentially monitor long-term heavy metal concentrations of chronically contaminated sites such as those on the Southern North Sea coast and beyond.

2. Materials and methods

2.1. Museum collection and sampling site

Nucella lapillus specimens were obtained from the Royal Belgian Institute of Natural Sciences, Brussels, Belgium (RBINS) collections. All the material used in this study and the preparations are kept at RBINS under loan number R.I.2919.03. These samples were collected between 1888 and 2019 on the Belgian and Dutch coasts from the port of Oostende (Belgium, 51°14'N 2°55'E) to the beach of Zoutelande (the Netherlands, 51°29'N 3°28'E), spanning a distance of about 49 km

Table 1

Sampling details of the *Nucella lapillus* shells used in this study. For each sampling location the number of shells, their respective mean height and standard deviation are reported. Only shells with clearly identifiable sampling location were used. Sampling locations are sorted by sampling year.

Sampling year	Sampling site	Storage conditions	Individuals	Mean shell height (mm)	Var. shell height (1σ)
1888	Blankenberge	Dry	4	26.1	0.5
1904	Zoutelande	Dry	3	31.7	2.0
1911	Zeebrugge	Ethanol	1	32.5	
1911	Zwarte Polder	Ethanol	1	32.7	
1928	Heist	Dry	2	27.0	2.0
1929	Zeebrugge	Ethanol	1	26.5	
1929	Zeebrugge	Ethanol	2	29.6	2.3
1932	Heist	Ethanol	3	29.3	2.6
1936	Duinbergen	Ethanol	2	26.7	1.1
1937	Blankenberge	Ethanol	2	26.6	0.4
1938	Zeebrugge	Ethanol	1	28.6	
1945	Heist	Ethanol	3	27.4	1.4
1946	Zeebrugge	Ethanol	1	27.8	
1946	Oostende	Ethanol	1	26.0	
1947	Zeebrugge	Ethanol	2	30.4	0.2
1948	Zeebrugge	Dry	1	27.1	
1967	Zeebrugge	Dry	3	26.6	2.5
1977	Zeebrugge	Dry	3	26.9	0.6
1978	Zeebrugge	Dry	3	31.1	0.7
2019	Zeebrugge	Fresh	3	33.1	2.7

(Table 1). Although, the Belgian and Dutch coasts are dominated by sandy beaches, which provide little hard substratum for *N. lapillus*, the extensive constructions of groynes, moles, and dikes against coastal erosion and flooding, have provided sufficient habitat for large populations in the Belgian and Dutch intertidal zone for centuries. Specimens had been preserved in either ethanol (70 %) filled glass jars or dried (flesh removed). In total, 42 *N. lapillus* specimens from seven adjacent sites were used for trace element analyses. These individuals had intact apices and showed no signs of internal or external dissolution or damage. The mean shell height of all samples was 28.7 ± 2.7 mm (1σ), and specimens were, therefore, likely at sexual maturity (Galante-Oliveira et al., 2010) when sampled. A detailed description of the archival collection is provided in Table 1. There were no archived samples between the late 1970s and 2019 because of the local loss of the species due to the extensive use of the organotin-compound tributyltin (TBT) from the 1970s (Kerckhof, 1988). TBT was used as an antifouling agent on the hulls of boats and causes imposex in *N. lapillus* (Gibbs et al., 1991; Oehlmann et al., 1998), a condition in which the female develops a vas deferens, hindering reproduction which led to the local extinction of *N. lapillus* on the Belgian coast (Kerckhof, 1988). The first report of a sparse recurrence of *N. lapillus* on the Belgian coast is from late 2012 (De Blauwe and d'Udekem d'Acoz, 2012).

2.2. Metal/Ca analysis

Epibionts like barnacles were removed from the shells using a scalpel before elemental analyses. Standard morphometric measurements of shell height, shell width, aperture height and aperture width were obtained using digital Vernier callipers (± 0.1 mm). Specimens were then sectioned perpendicular to the aperture opening along the mid-section of the last whorl using a diamond saw. The anterior side of each specimen was embedded in polyester resin (Kleer-Set FF, MetPrep, Coventry, UK), and all embedded shell sections were smoothed on silicon paper and subsequently polished following a stepwise polishing routine using diamond paste with the grain sizes six to one micron on an automated polishing rig. After polishing, samples were ultra-sonicated for 2 min, briefly rinsed in ultra-pure ethanol and subsequently rinsed with Milli-Q water to remove the polishing residue. Heavy metal analyses were carried out by laser-ablation multi-collector inductively coupled plasma mass spectrometry (LA-MC-ICP-MS) at GEOMAR, Helmholtz Centre of Ocean Research in Kiel, Germany. An ESI New Wave Research UP193FX excimer laser operating at 193 nm was used to ablate material from the shell sections connected to a Thermo Fisher (former VG) Axiom MC-ICP-MS. Fourteen specimens were simultaneously inserted into the laser's ablation cell. The order in which samples were ablated was randomised to avoid sampling bias. The Axiom was run at 1200 W, with 17 l min⁻¹ cool gas, 2.4 l min⁻¹ auxiliary gas and 1.1 l min⁻¹ sample gas (Argon) flow with robust plasma conditions identified by a normalised Argon index (NAI) of seven (Fietzke and Frische, 2015). The laser was operated in line scan mode with a 35 μm spot diameter, a fluence of 4.2 J cm⁻² and a scan velocity of 10 μm s⁻¹. The laser was set to a frequency of 10 Hz on the samples and 5 Hz on the standard. To convert count ratios to concentration ratios, the NIST610 soda-lime glass standard (National Institute of Standards and Technology, U.S. Department of Commerce: Gaithersburg, MD, USA) was measured alongside the samples.

The shell of *N. lapillus* consists of two distinct layers. On the outside, irregular prismatic calcite makes up 80 % of the total shell thickness; underneath this layer, crossed-lamellar aragonite lines the inside of the shell and the two layers may be separated by a transitional spherulitic layer (Mayk, 2020). Since trace element concentrations may vary between aragonite and calcite (Kitano et al., 1976), we decided to ablate material individually from both the shell aragonite and the calcite. However, since calcite makes up most of the shell thickness, a greater focus was put on the calcite. The material was ablated from near the aperture just behind the apertural teeth (Fig. 1). The ablation profiles were positioned to start in and follow the thin aragonite layer, then

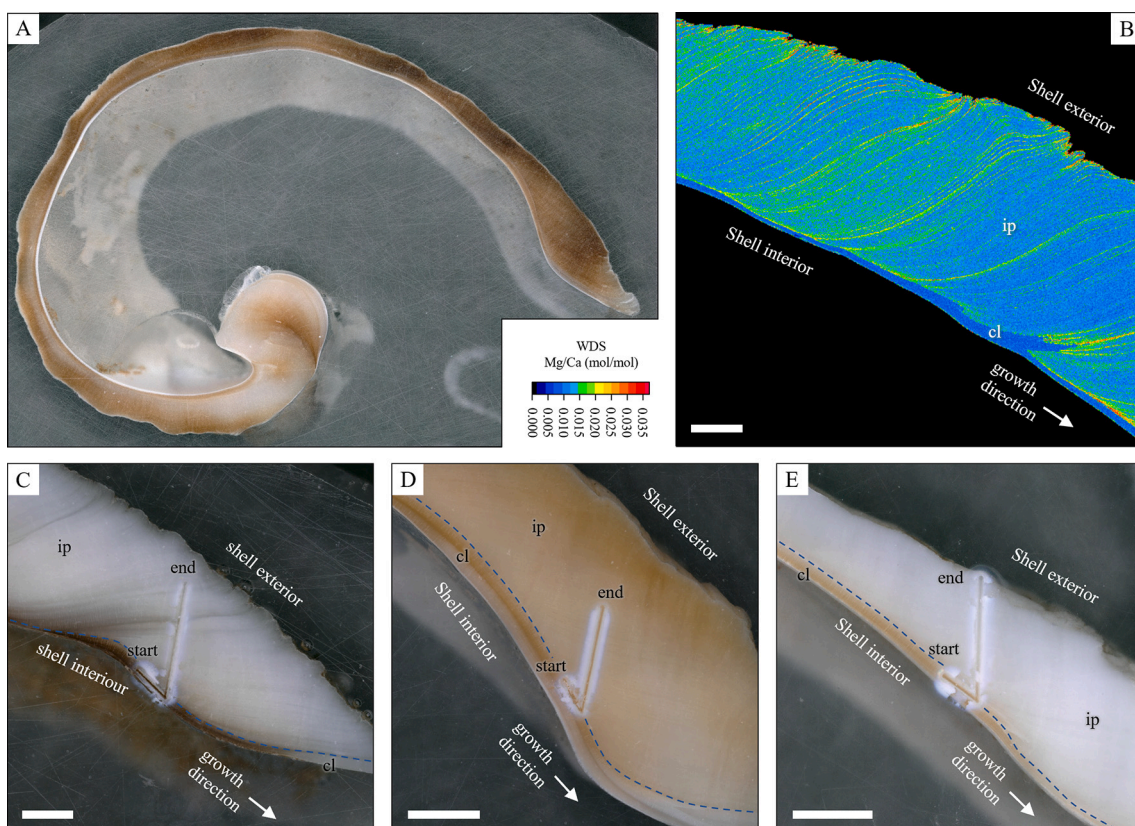


Fig. 1. Light microscope images of laser ablation lines. A. Light microscope overview of a shell section. B. Electron Microprobe image showing Mg/Ca ratios in the shell of a specimen to highlight individual growth bands and their orientation. C–E. Example images of three samples analysed in this study. Laser ablation line start and end are marked. cl: crossed-lamellar aragonite and ip: irregular prismatic calcite. Dotted lines represent the shell microstructure transition from ip to cl. Scale bars = 500 μm .

angle off into the calcite, moving from the interior to the shell's exterior. Following [Ekaratne and Crisp \(1982\)](#), we estimate that these samples encompassed approximately two weeks of shell growth. A common standard-sample bracketing sequence was used to identify and correct possible instrument drifts during the measurement sessions. Metal (Cu, Zn, Pb and Cd) counts were measured on electron multipliers, and calcium (Ca) counts were measured on Faraday cups. Three repeated measurements on the same ablation line were performed per sample for each metal, each bracketed by a line of Ca measurements. Every ablation profile was followed by at least 50 s of background signal collection (no laser firing).

For each sample, raw count data of Ca, Cu, Zn, Pb, and Cd were converted to Metal/Ca (= M/Ca) concentration ratios. First, ablation profiles were individually background corrected by subtracting the median background intensity of the last 35 s of each measurement from the respective ablation trend. Count values belonging to the aragonite and the calcite layers were separated, and M/Ca ratios were inferred from integrated, and background corrected count values. Thereafter, M/Ca count ratios were calibrated against M/Ca count ratios of the NIST610 standard to obtain M/Ca concentration ratios in $\mu\text{mol mol}^{-1}$. The “preferred” GeoRem database values for the elemental concentration in NIST610 were used for the calibration ([Jochum et al., 2011](#)). A 1.5 IQR outlier filter was applied to remove wild spikes from the data in a final step.

3. Results

Ca and Cu ablation profiles showed clear plateaus for analyses performed in the aragonite and calcite layers, whereas Zn and Pb ablation trends were more variable ([Fig. 2 A, C](#)). Elevated Cu, Zn and Pb counts

were observed frequently in the transition zone between the aragonite to the calcite layer ([Fig. 2](#)). Intensity spikes were sometimes observed at the end of the ablation profiles when approaching the outside of the shell. If present, these spikes occurred in all analysed elements (Ca, Cu, Zn, Pb, Cd), suggesting that they could be the result of surficial alteration (SA) of the outer calcite margin. In most cases, the remaining data were not affected by this and were used in the analyses after the intensity spikes were removed. No association between storage condition (wet or dry), sampling sites or sampling year and the occurrence of the intensity spikes was observed. Cd concentrations in both the aragonite and calcite layers were below the detection limits in all samples and were thus excluded from the report.

Shell Cu/Ca concentration ratios remained remarkably constant between 1888 and 2019 with a mean concentration of 1.25 ± 0.24 (1σ) $\mu\text{mol mol}^{-1}$ in the aragonite and 0.9 ± 0.22 (1σ) $\mu\text{mol mol}^{-1}$ in the calcite layer ([Fig. 3 A](#)). Shell Pb/Ca concentration ratios showed a pronounced increase in both the aragonite and calcite layers from 1888 until 1967 ([Fig. 3 B](#)) with shells collected in 1967 showing peak values at mean Pb/Ca concentration ratios of 0.09 ± 0.02 (1σ) $\mu\text{mol mol}^{-1}$ in the calcite layer, from where Pb/Ca concentration ratios dropped by an order of magnitude to a mean value of 0.009 ± 0.004 (1σ) $\mu\text{mol mol}^{-1}$ in 2019. There was no obvious trend in Zn/Ca ratios which remained relatively constant at mean values of 0.34 ± 0.49 (1σ) $\mu\text{mol mol}^{-1}$ in the aragonite and 0.29 ± 0.28 (1σ) $\mu\text{mol mol}^{-1}$ in the calcite layer ([Fig. 3 C](#)). Occasionally, individual shells exhibited higher Zn/Ca concentration ratios which did not follow an apparent trend.

Statistical comparisons of M/Ca concentration ratios between the aragonite and calcite layer (Supplementary Fig. 1) revealed that Cu/Ca concentration ratios were significantly higher in the aragonite than in the calcite layer (paired Wilcoxon: $V = 739$, $p < 0.001$) which is in line

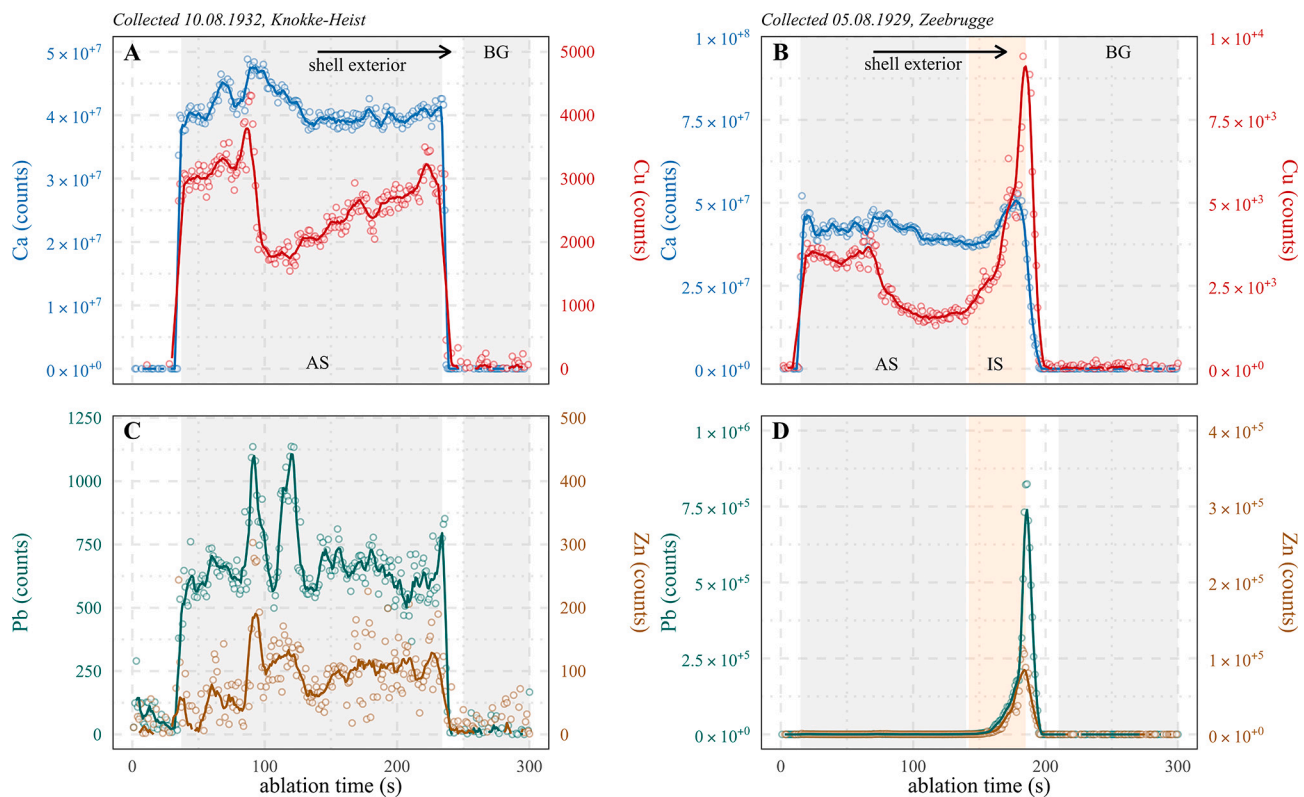


Fig. 2. Example ablation trends for Ca, Cu, Zn and Pb. Left panel shows ablation signal (AS) and background values (BG) for a *Nuccella lapillus* shell collected in 1932 at Knokke-Heist. Right panel, ablation trends for *N. lapillus* shell collected in 1929 at Zeebrugge showing distinct elevation in trace element counts (Cu, Zn and Pb) towards the outside of the shell suggesting a potential surficial alteration of the outer calcite margin. A. Ca and Cu counts and C. Pb and Zn counts of a specimen from 1932. B. Ca and Cu counts and D. Pb and Zn counts of a specimen from 1929 with pronounced posterior intensity spikes (IS) possibly due to surficial alteration. All count data shown are background corrected.

with experimental data (Fig. 4) (Kitano et al., 1976). Aragonite and calcite Cu/Ca concentration ratios also showed a significant linear relationship ($R^2 = 0.26$, $F_{(1,36)} = 14.22$, $p < 0.001$) (Fig. 5). Shell Pb/Ca concentration ratios were significantly higher in the calcite than in the aragonite layer (paired Wilcoxon: $V = 120$, $p = 0.02$), although the difference was not as well defined as it was for the Cu/Ca concentration ratios. Like Cu/Ca, Pb/Ca concentration ratios in the aragonite and calcite layers also showed a significant linear relationship ($R^2 = 0.46$, $F_{(1,28)} = 25.43$, $p < 0.001$) (Fig. 6 B). Zn/Ca concentration ratios in the calcite and aragonite layers showed no significant difference (paired Wilcoxon: $V = 208$, $p = 0.3$) and showed no linear relationship ($R^2 = -0.03$, $F_{(1,30)} = 0.21$, $p = 0.65$). Overall, no significant relationships among analysed M/Ca concentration ratios in the calcite or the aragonite layers were observed (Supplementary Figs. 2 and 3). Furthermore, no relationships of M/Ca with any of the analysed morphometric parameters were detected, suggesting that shell-bound heavy metal concentrations are largely unrelated to specimen size (within the limits of the specimen sizes studied here).

4. Discussion

There are several known pathways through which heavy metals are accumulated, and internal concentrations are regulated by *N. lapillus*. However, these pathways and their impact on internal heavy metal levels may not be congenial for all elements and, therefore, likely exert a significant influence on shell-bound heavy metal concentrations. Fig. 5 shows a simplified schematic representation of these and highlights the most likely pathways of heavy metals from the source into the shell of *N. lapillus*. Following their introduction into the marine environment, heavy metals take up different forms or speciations (e.g., dissolved, particulate or complexed forms) (Diop et al., 2014; González et al.,

2007). Heavy metals are transported along trophic gradients in the food chain, which in the case of *N. lapillus* was identified as a major source of metals in the soft tissue (Young, 1977). Although a general bioaccumulation effect of heavy metals in marine organisms has been contested, there is good evidence for a bio-magnification of metals in benthic food chains and especially those with gastropods as top predators (Wang, 2002), suggesting that historical contamination patterns are likely more pronounced in the predatory gastropod *N. lapillus* than in its prey. In addition, direct uptake of heavy metals from seawater into the calcifying fluid (from which the shell is precipitated) is also an important pathway, as the calcifying fluid is usually perceived to stand more or less in direct exchange with seawater. From Fig. 5, it is obvious that a direct uptake of heavy metals into the calcifying fluid represents the most desirable pathway in terms of environmental reconstruction, as it reflects the closest representation of the in situ environmental condition. However, since several other pathways can play a significant role, and some of the more common pollutant metals such as Zn also function as important metabolites (Vallee and Auld, 1990), the question arises as to how far shell-bound heavy metals in *N. lapillus* are a true depiction of environmental conditions or artefacts of trophic and internal processes.

Our analyses revealed that between 1888 and 2019, shell-bound Pb/Ca concentration ratios increased steadily from what can be considered “background levels” in 1888 to peak values in 1967. From 1967 this trend was reversed so that Pb/Ca levels decreased to background levels by 2019. Considering that we analysed multiple individual shells from multiple collection sites, this trend correlates remarkably well with recorded emission rates of leaded petrol in Europe over the same period (Fig. 6). A similar Pb trend has also been reported in *Arctica islandica* specimens from sites near Helgoland in the North Sea – a region approx. 430 km to the northeast of this study’s sampling site (Krause-Nehring et al., 2012). Given the large differences in location and habitat, and that

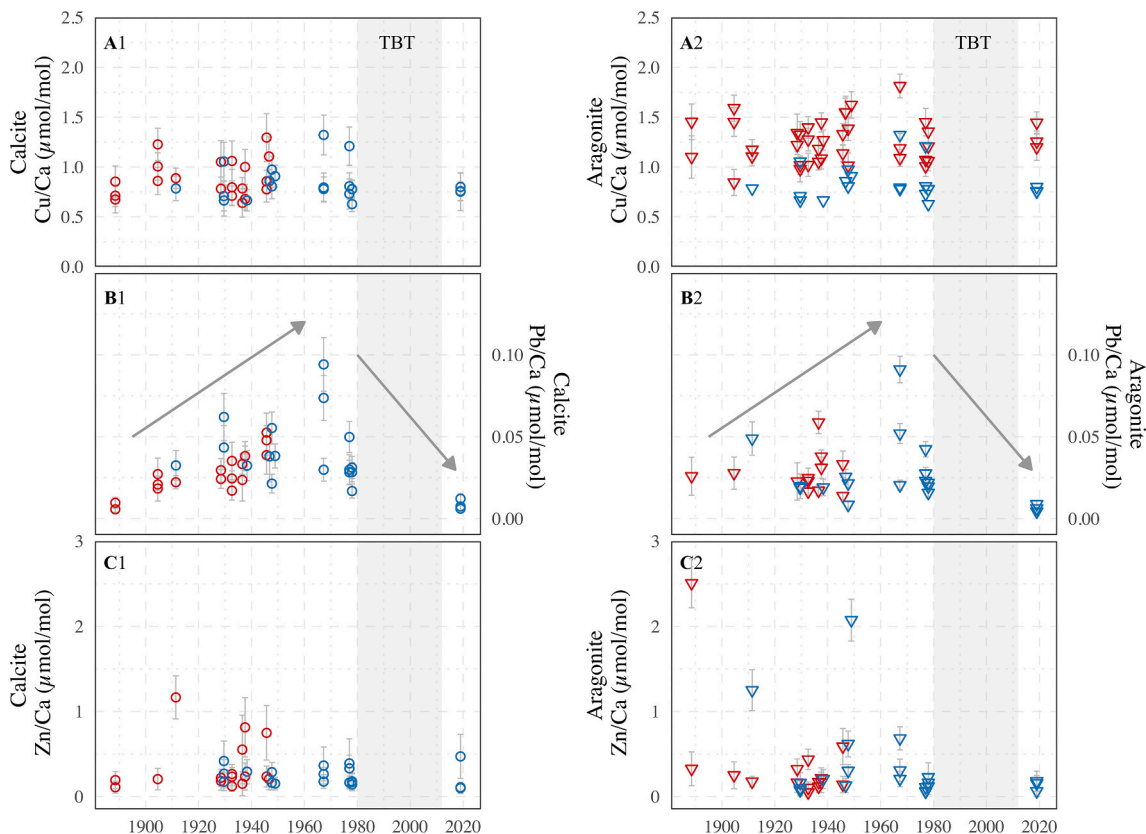


Fig. 3. Mean M/Ca in *Nucella lapillus* encompassing a period of 130 years from 1888 until 2019. A. Mean Cu/Ca concentration ratios in the calcite and aragonite layers. B. Mean Pb/Ca concentration ratios in the calcite and aragonite layers. Grey arrows mark Pb/Ca concentration increases until the 1970s from when it rapidly decreased. C. Mean Zn/Ca concentration ratios in the calcite and aragonite layers. Error bars represent one standard deviation. The grey area represents the time when *N. lapillus* was locally extinct due to the use of the organotin-compound tributyltin (TBT). Blue colour represents measurements of individuals collected from Zeebrugge; red colour refers to individuals collected at the other sampling sites (refer to Table 1). (For interpretation of the references to colour in this figure legend, the reader is referred to the web version of this article.)

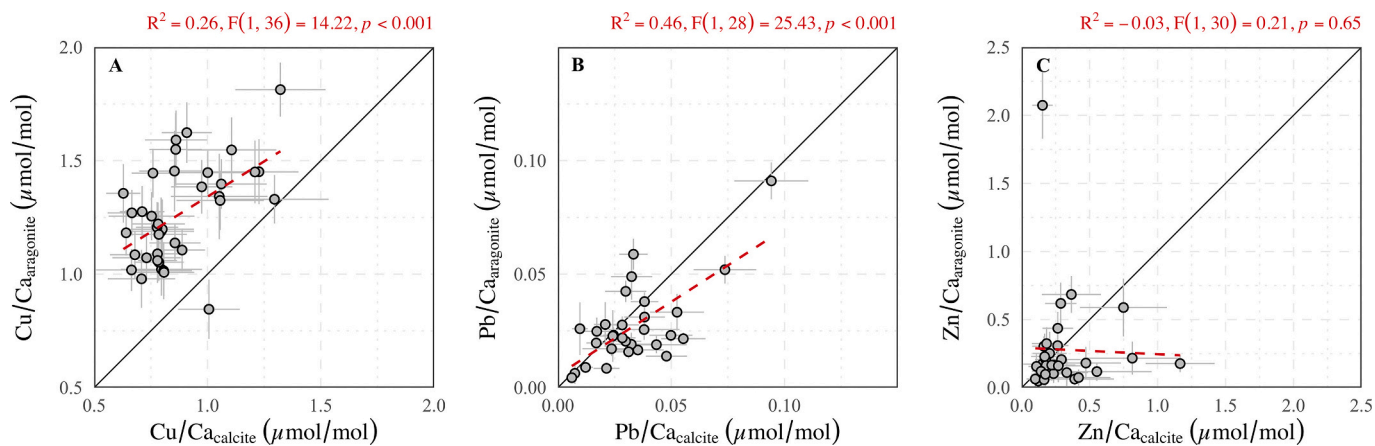


Fig. 4. Pairwise comparison of mean M/Ca ratios in the calcite and aragonite layers of *Nucella lapillus*. A. Pairwise comparison of mean Cu/Ca concentration ratios. B. Pairwise comparison of mean Pb/Ca concentration ratios. C. Pairwise comparison of mean Zn/Ca concentration ratios. Error bars represent one standard deviation. Solid lines represent the 1:1 line between calcite and aragonite. Red dashed lines represent linear regression lines through all data points. Linear regression summaries are provided above each plot. (For interpretation of the references to colour in this figure legend, the reader is referred to the web version of this article.)

A. islandica can live for over 500 years (Butler et al., 2013) compared to the <10 years lifespan of *N. lapillus* (Feare, 1970), plus the differences in growth rates and nutrition, the similarities in Pb trends appear remarkable and suggest a direct coupling of shell-bound to environmental Pb concentrations, driven by a history of widespread anthropogenic Pb emission. Indeed, global emissions of leaded petrol have a long history of environmental pollution that only recently came to an end.

With Algeria's ban on leaded petrol in July 2021, the UN finally could declare the “Era of leaded petrol over”. Although a significant anthropogenic fingerprint of Pb emissions from coal combustion already existed since the 1850s (Kelly et al., 2009), it was not until the 1920s that Pb was emitted in large quantities into the environment. Since 1922, tetraethyl lead was used as a petrol additive to enhance engine performance, later deemed a “catastrophe for the environment and

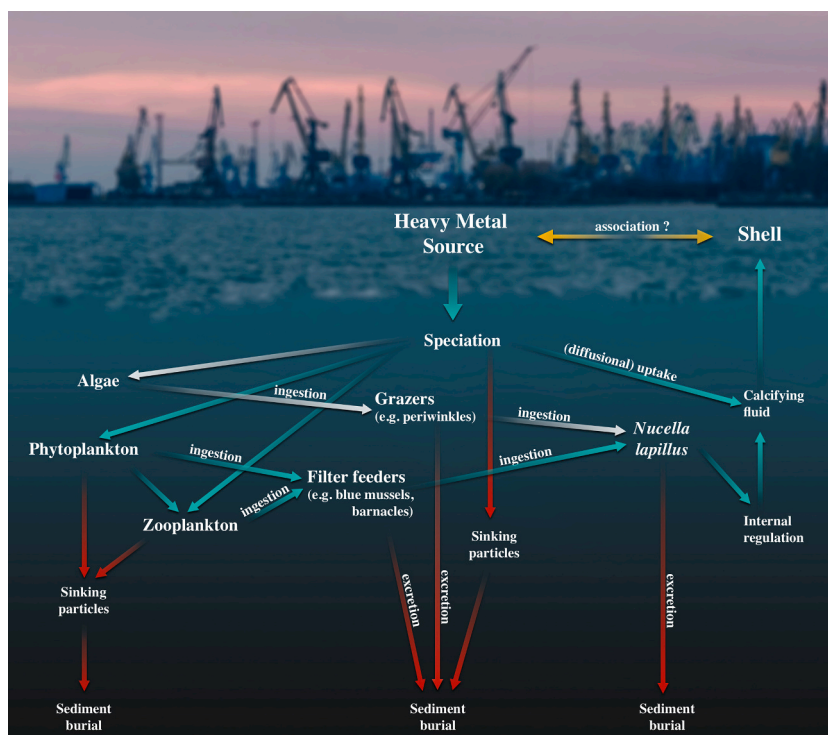


Fig. 5. Schematic representation of potential heavy metal pathways along trophic gradients from the source into the shell of *Nucella lapillus*.

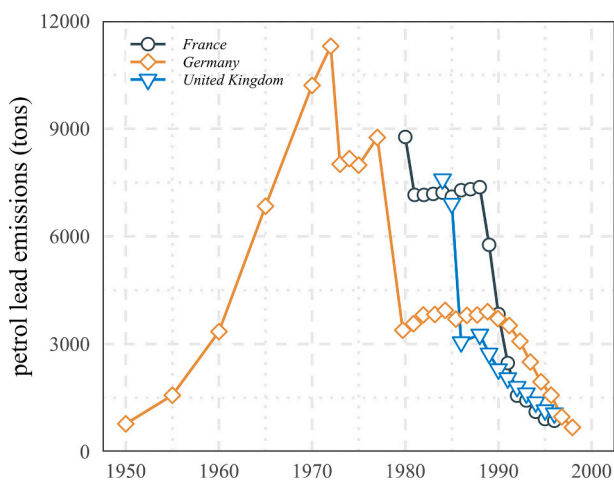


Fig. 6. Lead emissions from petrol use of the three main emitting countries in Europe between 1950 and 1999. Data were obtained from Hagner (1999) and sources therein.

public health" (Landrigan, 2002). In the 1960s, Pb pollution became a global concern. It was discovered that car exhaust emissions were the main source of Pb pollution in the environment and that much of the population in Europe was chronically exposed to severely elevated Pb levels (Patterson, 1965). These emissions peaked around the 1970s (Fig. 6) around the same time when shell-bound Pb/Ca concentration ratios peaked in the *N. lapillus* shells analysed in this study and required legislation to address the issue of environmental Pb pollution. Germany was among the first European countries with large Pb emission rates that passed new regulations in 1971, legislating for a gradual reduction in petrol Pb content (Hagner, 1999). At the European level, this was initiated seven years later, but it was not until 1989 before unleaded 95 octane petrol became the recommended standard (Hagner, 1999). These legislative interventions significantly impacted the environment, as

shown by long-term marine and riverine monitoring studies. On the southern North Sea coast, a significant reduction of atmospheric Pb concentrations by 86 % and aquatic Pb levels by 42 % from 1985 until 2000 (Gao et al., 2013) were recorded, underpinning the relationship between the archival *N. lapillus* Pb/Ca trends presented here and environmental Pb pollution levels.

Unlike Pb/Ca, Cu/Ca concentration ratios in the shell of *N. lapillus* remained stable with mean values of 1.25 ± 0.24 (1σ) $\mu\text{mol mol}^{-1}$ in the aragonite and 0.9 ± 0.22 (1σ) $\mu\text{mol mol}^{-1}$ in the calcite layer between 1888 and 2019 (Fig. 3). These results do not reflect global emission trends as environmental Cu concentrations have changed markedly over the last century. For example, studies of ice/snow core records from the Swiss Alps from the 1650s to 2000 revealed that atmospheric Cu concentrations increased significantly to peak values towards the end of the 20th century (Barbante et al., 2004). Similar trends were also reported from the Baltic Sea (Shahabi-Ghahfarokhi et al., 2021). In addition, local long-term monitoring revealed that aquatic Cu concentrations decreased by 47 % between 1985 and 2000 in the Scheldt Estuary and Belgian coastal zone (Gao et al., 2013). However, despite these significant trend changes, shell-bound Cu/Ca concentration ratios in *N. lapillus* seemed unaffected. Similarly, shell-bound Zn/Ca concentration ratios also remained unaffected by global Zn emission. Analyses of ice/snow cores from the Swiss Alps showed a steady increase in atmospheric Zn concentration since the late 19th century - with concentrations in 2000 being 12 times higher than in 1890 (Barbante et al., 2004). In addition, seawater measurements in the Scheldt Estuary showed decreasing Zn concentrations between 1978 and 2010 in both particulate ($350 \mu\text{g g}^{-1}$ to $86 \mu\text{g g}^{-1}$) and dissolved ($6.5 \mu\text{g l}^{-1}$ to $1.7 \mu\text{g l}^{-1}$) fractions (Gao et al., 2013). Together, these reports suggest a pronounced trend history of environmental Zn concentration similar to that reported for Pb or Cu. However, despite this pronounced environmental trend, Zn/Ca concentration ratios in the analysed archival *N. lapillus* shells remained relatively stable throughout the last 130 years.

5. Conclusion

To summarise, heavy metal concentrations in *N. lapillus* shell appear to reflect different environmental and organism-controlled constraints, leading to very different responses in shell-bound heavy metal concentrations to environmental gradients. Both Cu/Ca and Zn/Ca concentration ratios remained remarkably stable within the shell of *N. lapillus* despite significant changes in environmental concentrations between 1888 and 2019 on the Southern North Sea coast. In contrast, Pb/Ca concentration ratios in *N. lapillus* shells closely resembled reported environmental Pb concentration trends thereby reflecting the anthropogenic history of the use of lead in petrol in Europe. Our results show that shell-bound Pb concentrations made a full return to baseline levels after peak Pb pollution levels in the 1960s–1970s most probably as a result of successful Pb emission management, which can be considered a success of past legislative efforts and motivation for future conservation efforts. Overall, it can be concluded that archival *N. lapillus* shells are likely suitable for Pb monitoring but unsuitable for Cu and Zn monitoring of chronic long-term pollution in the intertidal zone.

CRedit authorship contribution statement

D.M., E.M.H., J.F., T.B., and L.S.P. conceived the original project; D.M. sampled the museum collections; D.M. and J.F. analysed the samples; T.B. provided the archival specimens and collected the living specimens; D.M. wrote the first draft of the manuscript, and all co-authors contributed substantially to revisions.

Declaration of competing interest

The authors declare that they have no known competing financial interests or personal relationships that could have appeared to influence the work reported in this paper.

Data availability

Data will be made available on request.

Acknowledgements

We are indebted to Dr. Yves Samyn, curator of the invertebrate collections of RBINS for allowing us to study the archival *Nucella lapillus* material under his care. This study was supported by a NERC studentship awarded to DM (NE/L002507/1).

Appendix A. Supplementary data

Supplementary data to this article can be found online at <https://doi.org/10.1016/j.marpolbul.2022.114286>.

References

- Baeyens, W., 1997. Evolution of trace metal concentrations in the scheldt estuary (1978–1995). A comparison with estuarine and ocean levels. *Hydrobiologia* 366, 157–167. <https://doi.org/10.1023/A:1003136613574>.
- Barbante, C., Schwikowski, M., Döring, T., Gäggeler, H.W., Schotterer, U., Tobler, L., van de Velde, K., Ferrari, C., Cozzi, G., Turetta, A., Rosman, K., Bolshov, M., Capodaglio, G., Cescon, P., Boutron, C., 2004. Historical record of european emissions of heavy metals to the atmosphere since the 1650s from alpine snow/ice cores drilled near Monte Rosa. *Environ. Sci. Technol.* 38, 4085–4090. <https://doi.org/10.1021/es049759r>.
- Boehnert, S., Birkelund, A.R., Schmiedl, G., Kuhnert, H., Kuhn, G., Hass, H.C., Hebbeln, D., 2020. Test deformation and chemistry of foraminifera as response to anthropogenic heavy metal input. *Mar. Pollut. Bull.* 155, 111112 <https://doi.org/10.1016/j.marpolbul.2020.111112>.
- Burrows, M.T., Hughes, R.N., 1989. Natural foraging of the dogwhelk, *Nucella lapillus* (Linnaeus); the weather and whether to feed. *J. Molluscan Stud.* 55, 285–295. <https://doi.org/10.1093/mollus/55.2.285>.
- Butler, P.G., Wanamaker, A.D., Scourse, J.D., Richardson, C.A., Reynolds, D.J., 2013. Variability of marine climate on the north icelandic shelf in a 1357-year proxy archive based on growth increments in the bivalve *Arctica islandica*. *Palaeogeogr. Palaeoclimatol. Palaeoecol.* 373, 141–151. <https://doi.org/10.1016/j.palaeo.2012.01.016>.
- Camphuysen, K., Vollaard, B., 2016. Oil pollution in the Dutch sector of the North Sea. In: Carpenter, A. (Ed.), *Oil Pollution in the North Sea*. Springer International Publishing, Cham, pp. 117–140. <https://doi.org/10.1007/978-2015-430>.
- Chitrakar, P., Baawain, M.S., Sana, A., Al-Mamun, A., 2019. Current status of marine pollution and mitigation strategies in arid region: a detailed review. *Ocean Sci. J.* 54, 317–348. <https://doi.org/10.1007/s12601-019-0027-5>.
- CIESIN, 2012. National aggregates of geospatial data collection: Population, landscape, and climate estimates, version 3 (PLACE III). <https://doi.org/10.7927/H4F769GP>.
- De Blauwe, H., d'Udekem d'Acoz, 2012. Voortplantende populatie van de purperslak (*Nucella lapillus*) in België na meer dan 30 jaar afwezigheid (Mollusca, gastropoda, Muricidae). *De Strandvlo* 32, 127–131.
- Dethlefsen, V., 1988. Status report on aquatic pollution problems in Europe. *Aquat. Toxicol.* 11, 259–286. [https://doi.org/10.1016/0166-445X\(88\)90078-1](https://doi.org/10.1016/0166-445X(88)90078-1).
- Diop, C., Dewaelé, D., Diop, M., Touré, A., Cabral, M., Cazier, F., Fall, M., Diouf, A., Ouddane, B., 2014. Assessment of contamination, distribution and chemical speciation of trace metals in water column in the dakar coast and the saintlouis estuary from senegal, west africa. *Mar. Pollut. Bull.* 86, 539–546. <https://doi.org/10.1016/j.marpolbul.2014.06.051>.
- Ekaratne, S.U.K., Crisp, D.J., 1982. Tidal micro-growth bands in intertidal gastropod shells, with an evaluation of band-dating techniques. *Proc. R. Soc. Lond. B* 214, 305–323. <https://doi.org/10.1098/rspb.1982.0013>.
- Feare, C.J., 1970. Aspects of the ecology of an exposed shore population of dogwhelk *Nucella lapillus* (L.). *Oecologia* 5, 1–18. <https://doi.org/10.1007/BF00345973>.
- Fergusson, J.E., 1990. *The heavy elements: chemistry, environmental impact and health effects*. Elsevier Science Limited.
- Fietzke, J., Frische, M., 2015. Experimental evaluation of elemental behavior during LA-ICP-MS: influences of plasma conditions and limits of plasma robustness. *J. Anal. At. Spectrom.* 31, 234–244. <https://doi.org/10.1039/C5JA00253B>.
- Galante-Oliveira, S., Oliveira, I., Santos, J.A., Pacheco, M., Barroso, C.M., Pereira, M.de L., 2010. Factors affecting RPSI in imposex monitoring studies using *Nucella lapillus* (L.) as bioindicator. *J. Environ. Monit.* 12, 1055–1063. <https://doi.org/10.1039/b921834c>.
- Gao, Y., de Brauwere, A., Elskens, M., Croes, K., Baeyens, W., Leermakers, M., 2013. Evolution of trace metal and organic pollutant concentrations in the Scheldt River basin and the belgian coastal zone over the last three decades. *J. Mar. Syst.* 128, 52–61. <https://doi.org/10.1016/j.jmarsys.2012.04.002>.
- Gibbs, P.E., Bryan, G.W., Pascoe, P.L., 1991. TBT-induced imposex in the dogwhelk, *Nucella lapillus*: geographical uniformity of the response and effects. *Mar. Environ. Res.* 32, 79–87. [https://doi.org/10.1016/0141-1136\(91\)90035-7](https://doi.org/10.1016/0141-1136(91)90035-7).
- González, I., Jordán, M.M., Sanfeliu, T., Quiroz, M., de la Fuente, C., 2007. Mineralogy and heavy metal content in sediments from rio gato, carelmapu and cucao, southern Chile. *Environ. Geol.* 52, 1243–1251. <https://doi.org/10.1007/s00254-006-0562-0>.
- Gu, Y.-G., 2018. Heavy metal fractionation and ecological risk implications in the intertidal surface sediments of Zhelin Bay, South China. *Mar. Pollut. Bull.* 129, 905–912. <https://doi.org/10.1016/j.marpolbul.2017.10.047>.
- Hagner, C., 1999. *Historical Review of European Gasoline Lead Content Regulations and their Impact on German Industrial Markets*. GKSS Research Center, Germany.
- Holland, H.A., Schöne, B.R., Marali, S., Jochum, K.P., 2014. History of bioavailable lead and iron in the greater north sea and iceland during the last millennium - a bivalve sclerochronological reconstruction. *Mar. Pollut. Bull.* 87, 104–116. <https://doi.org/10.1016/j.marpolbul.2014.08.005>.
- Jochum, K.P., Weis, U., Stoll, B., Kuzmin, D., Yang, Q., Raczek, I., Jacob, D.E., Stracke, A., Birbaum, K., Frick, D.A., Günther, D., Enzweiler, J., 2011. Determination of reference values for NIST SRM 610–617 glasses following ISO guidelines. *Geostand. Geoanal. Res.* 35, 397–429. <https://doi.org/10.1111/j.1751-908x.2011.00120.x>.
- Kelly, A.E., Reuter, M.K., Goodkin, N.F., Boyle, E.A., 2009. Lead concentrations and isotopes in corals and water near Bermuda, 1780–2000. *Earth Planet. Sci. Lett.* 283, 93–100. <https://doi.org/10.1016/j.epsl.2009.03.045>.
- Kerckhof, F., 1988. Over het verdwijnen van de purperslak *Nucella lapillus* (Linnaeus, 1758), langs onze kust. *De Strandvlo* 8, 82–85.
- Kitano, Y., Kanamori, N., Yoshioka, S., 1976. Adsorption of zinc and copper ions on calcite and aragonite and its influence on the transformation of aragonite to calcite. *Geochem. J.* 10, 175–179. <https://doi.org/10.2343/geochemj.10.175>.
- Knopf, B., Fliedner, A., Radermacher, G., Rüdell, H., Paulus, M., Pirntke, U., Koschorreck, J., 2020. Seasonal variability in metal and metalloid burdens of mussels: using data from the german environmental specimen bank to evaluate implications for long-term mussel monitoring programs. *Environ. Sci. Eur.* 32, 1–13. <https://doi.org/10.1186/s12302-020-0289-7>.
- Krause-Nehring, J., Brey, T., Thorrold, S.R., 2012. Centennial records of lead contamination in northern Atlantic bivalves (*Arctica islandica*). *Mar. Pollut. Bull.* 64, 233–240. <https://doi.org/10.1016/j.marpolbul.2011.11.028>.
- Landrigan, P.J., 2002. The worldwide problem of lead in petrol. *Bull. World Health Organ.* 80, 768.
- Liu, Q., Liao, Y., Shou, L., 2018. Concentration and potential health risk of heavy metals in seafoods collected from sanmen bay and its adjacent areas. *China. Mar. Pollut. Bull.* 131, 356–364. <https://doi.org/10.1016/j.marpolbul.2018.04.041>.
- Mayk, D., 2020. Transitional spherulitic layer in the muricid *Nucella lapillus*. *J. Molluscan Stud.* 87 <https://doi.org/10.1093/mollus/eyaa035>.
- Mayk, D., Peck, L.S., Harper, E.M., 2022. Evidence for carbonate system mediated shape shift in an intertidal predatory gastropod. *Front. Mar. Sci.* 9 <https://doi.org/10.3389/fmars.2022.894182>.

- Morgan, P.R., 1972. The influence of prey availability on the distribution and predatory behaviour of *Nucella lapillus* (L.). *J. Anim. Ecol.* 41, 257–274. <https://doi.org/10.2307/3468>.
- Oehlmann, J., Bauer, B., Minchin, D., Schulte-Oehlmann, U., Fioroni, P., Markert, B., 1998. Imposex in *Nucella lapillus* and intersex in *Littorina littorea*: Interspecific comparison of two TBT-induced effects and their geographical uniformity. In: O'Riordan, R.M., Burnell, G.M., Davies, M.S., Ramsay, N.F. (Eds.), *Aspects of Littorinid Biology*. Springer Netherlands, Dordrecht, pp. 199–213. <https://doi.org/10.1007/978-94-011-5336-2/22>.
- Oron, S., Sadekov, A., Katz, T., Goodman-Tchernov, B., 2021. Benthic foraminifera geochemistry as a monitoring tool for heavy metal and phosphorus pollution - a post fish-farm removal case study. *Mar. Pollut. Bull.* 168, 112443 <https://doi.org/10.1016/j.marpolbul.2021.112443>.
- Patterson, C.C., 1965. Contaminated and natural lead environments of man. *Arch. Environ. Health* 11, 344–360. <https://doi.org/10.1080/00039896.1965.10664229>.
- Ragi, A.S., Leena, P.P., Cheriyan, E., Nair, S.M., 2017. Heavy metal concentrations in some gastropods and bivalves collected from the fishing zone of South India. *Mar. Pollut. Bull.* 118, 452–458. <https://doi.org/10.1016/j.marpolbul.2017.03.029>.
- Shahabi-Ghahfarokhi, S., Åström, M., Josefsson, S., Apler, A., Ketzer, M., 2021. Background concentrations and extent of Cu, As, Co, and U contamination in Baltic Sea sediments. *J. Sea Res.* 176, 102100 <https://doi.org/10.1016/j.seares.2021.102100>.
- Silva, C.P. da, da Silveira, E.L., de Campos, S.X., 2017. Environmental pollution by heavy metals in the São João river basin, southern Brazil. *Environ. Earth Sci.* 76, 554. <https://doi.org/10.1007/s12665-017-6890-4>.
- Tchounwou, P.B., Yedjou, C.G., Patlolla, A.K., Sutton, D.J., 2012. Heavy metal toxicity and the environment. *Experientia Suppl.* 101, 133–164. <https://doi.org/10.1007/978-3-7643-8340-4/6>.
- Titelboim, D., Sadekov, A., Blumenfeld, M., Almogi-Labin, A., Herut, B., Halicz, L., Benalabet, T., Torfstein, A., Kucera, M., Abramovich, S., 2021. Monitoring of heavy metals in seawater using single chamber foraminiferal sclerochronology. *Ecol. Indic.* 120, 106931 <https://doi.org/10.1016/j.ecolind.2020.106931>.
- Titelboim, D., Sadekov, A., Hyams-Kaphzan, O., Almogi-Labin, A., Herut, B., Kucera, M., Abramovich, S., 2018. Foraminiferal single chamber analyses of heavy metals as a tool for monitoring permanent and short term anthropogenic footprints. *Mar. Pollut. Bull.* 128, 65–71. <https://doi.org/10.1016/j.marpolbul.2018.01.002>.
- Trussell, G.C., Ewanchuk, P.J., Bertness, M.D., 2003. Trait-mediated effects in rocky intertidal food chains: predator risk cues alter prey feeding rates. *Ecology* 84, 629–640. [https://doi.org/10.1890/0012-9658\(2003\)084%5B0629::tmeiri%5D2.0.co;2](https://doi.org/10.1890/0012-9658(2003)084%5B0629::tmeiri%5D2.0.co;2).
- Vallee, B.L., Auld, D.S., 1990. Zinc coordination, function, and structure of zinc enzymes and other proteins. *Biochemistry* 29, 5647–5659. <https://doi.org/10.1021/bi00476a001>.
- Van Alsenoy, V., Bernard, P., Van Grieken, R., 1993. Elemental concentrations and heavy metal pollution in sediments and suspended matter from the Belgian North Sea and the scheldt estuary. *Sci. Total Environ.* 133, 153–181. [https://doi.org/10.1016/0048-9697\(93\)90119-Q](https://doi.org/10.1016/0048-9697(93)90119-Q).
- Verwey, J., 1915. *De trekvogels, de oorlog en nog wat*. *Levende Natuur* 20, 20.
- Wang, W.X., 2002. Interactions of trace metals and different marine food chains. *Mar. Ecol. Prog. Ser.* 243, 295–309. <https://doi.org/10.3354/meps243295>.
- Young, M.L., 1977. The roles of food and direct uptake from water in the accumulation of zinc and iron in the tissues of the dogwhelk, *Nucella lapillus* (L.). *J. Exp. Mar. Biol. Ecol.* 30, 315–325. [https://doi.org/10.1016/0022-0981\(77\)90039-9](https://doi.org/10.1016/0022-0981(77)90039-9).
- Zoumis, T., Schmidt, A., Grigorova, L., Calmano, W., 2001. Contaminants in sediments: remobilisation and demobilisation. *Sci. Total Environ.* 266, 195–202. [https://doi.org/10.1016/S0048-9697\(00\)00740-3](https://doi.org/10.1016/S0048-9697(00)00740-3).
- Zwolsman, J.J.G., Van Eck, B.T.M., Van Der Weijden, C.H., 1997. Geochemistry of dissolved trace metals (cadmium, copper, zinc) in the scheldt estuary, southwestern Netherlands: impact of seasonal variability. *Geochim. Cosmochim. Acta* 61, 1635–1652. [https://doi.org/10.1016/S0016-7037\(97\)00029-X](https://doi.org/10.1016/S0016-7037(97)00029-X).